Int. J. Electrochem. Sci., 4 **(2009)** 1436 - 1451

International Journal of ELECTROCHEMICAL SCIENCE
www.electrochemsci.org

A Comparative Study of Carbon Nanotube paste Electrode for Development of Indicator-free DNA Sensors Using DPV and EIS: Human Interleukin-2 Oligonucleotide as a Model

Jahan-Bakhsh Raoof[1,*], *Mohammad Saeid Hejazi* [2,3], *Reza Ojani*[1], *Ezat Hamidi Asl*[1]

[1] Eletroanalytical Chemistry Research Laboratory, Analytical Chemistry Department of Faculty of Chemistry, Mazandran University, Babolsar, Iran
[2] Faculty of Pharmacy, Tabriz University of Medical Sciences, Tabriz, Iran
[3] Drug Applied and Pharmaceutical Nonotechnology Research Center, Tabriz University of Medical Sciences, Tabriz, Iran
[*]E-mail: j.raoof@umz.ac.ir

Received: 30 August 2009 / *Accepted:* 15 October 2009 / *Published:* 11 November 2009

Differential pulse voltammetry (DPV) and electrochemical impedance spectroscopy (EIS) were employed for development of electrochemical DNA hybridization biosensors based on carbon paste electrode (CPE) and multi-wall carbon nanotubes incorporated into carbon paste electrode (CNTPE). The sensors rely on immobilization of a 20-mer single stranded oligonucleotide (chIL-2) probe for detection of target DNA, as a model. The hybridization event was compared by DPV and EIS. Result showed that employment of EIS for detection of hybridization on CNTPE surface was impossible and on CPE surface was not beneficial. However, DPV method demonstrated a proper potential for detection of hybridization event on the surface of the electrodes. Moreover, CNTPE showed some advantages over CPE. Accordingly, further studies including CNTPE electrochemical pretreatment effect on probe adsorption, probe immobilization conditions including potential and time as well as selectivity of the biosensor were carried out using DPV method and optimum conditions were suggested.

Keywords: Human interleukine-2 gene; Carbon nanotubes paste electrode; Differential pulse voltammetry; Electrochemical impedance spectroscopy; Indicator-free DNA determination

1. INTRODUCTION

Nucleic acid hybridization has become a fundamental technique in molecular biology for detection and analysis of specific DNA sequences. Such analysis plays a significant role in many areas including clinical diagnosis, forensic and environmental analysis and monitoring of food quality [1].

DNA biosensors consist of a biological recognition layer, usually single stranded DNA and a transducer converting the recognition event into a measurable signal. Optical, piezoelectric or electrochemical instruments are often used in DNA biosensors as transducers [2-4]. Electrochemical methods, in particular, provide sensitive, cost effective and rapid way of analysis [5, 6]. The detection is accomplished by immobilization of single stranded DNA onto electrode surface and hybridization of a target DNA sequence present in the sample. The method is very efficient and specific, because DNA sensor can detect an analyte even in the presence of a mixture of many different nucleic acid fragments [7].

Electrochemical detection of DNA hybridization is carried out with two indirect and direct methods. Indirect methods are based on the determination of electroactive indicators whose interaction and association level with double-stranded and single-stranded DNAs are quite different. Electroactive indicators include anticancer agents [8], organic dyes [9] and metal complexes [10]. Direct methods are mainly related to the intrinsic electrochemical activity of the nucleobases such as guanine and adenine [11]. Direct DNA hybridization detection strategy is also called label-free or indicator-free detection.

Development of DNA electrochemical sensors is highly conditioned by construction of suitable working electrodes [12]. Among different kinds of working electrodes, carbon paste electrodes are particularly popular [13]. Very often they are modified by some compounds such as carbon nanotubes (CNTs) incorporated into the electrode [14].

Some years after discovery of fullerenes [15], Iijima [16] reported the synthesis of a new carbon material, the carbon nanotubes. Since then, CNTs have received enormous attention due to their unique structural, electronic, mechanical, and chemical properties [17].

The unique electrocatalytic properties of CNTs make them extremely attractive for the task of electrochemical sensing. Electrodes modified with CNTs have been employed for detection of important biomolecules including cytochrome C, ascorbic acid, NADH, etc. [18]. Wide ranges of inorganic and biological molecules can be adsorbed onto nanotubes in the hope of using them as highly accurate tiny sensors [18]. CNTs have been recently used as transducers for enhanced electrical detection of DNA hybridization [19]. The SP^2 hybridization and the outstanding electronic properties of nanotube coupled with their specific recognition properties of immobilized system indeed make CNTs, as ideal biosensors [20].

Electrochemical impedance spectroscopy is a method of measuring the impedance value of the electrode surface during the process of frequency variation. EIS is able to offer various properties of interface of the electrode and solution, including the electrode impedance, capacity of the electric double layer, and the surface electron transfer resistance (R_{ct}). This technology was used to characterize a DNA hybridization sensor to realize sensitive indicator–free detection of the gene sequences [21, 22]. Hybridization reaction of DNA on the electrode surface results in changing the R_{ct} value upon formation of duplex between probe and target DNA. The quantity of the negative charge on the surface of the electrode increases greatly due to hybridization formation and thus further impeding of the electron transfer of electrochemical active substances with negative charge such as $[Fe(CN)_6]^{3-/4-}$ at the electrode surface is observed. Therefore, the hybridization of DNA could be characterized via the R_{ct} enhancement [23].

Recently, we had developed several electrochemical DNA biosensor on the basis of human IL-2 gene using methylene blue as an electroactive label [24], with label –free method using a non-inosine substituted probe [25, 26], IL-2 corresponding oligonucleotide chain adopted for detection of IL-2 encoding DNA (PCR-amplified sample), [27] and recombinant DNAs (plasmids encoding human IL-2) [28]. Now, in this paper, we are reporting a carbon nanotubes paste electrode (CNTPE) indicator-free DNA biosensor for detection of short DNA sequences related to human interleukin-2 gene (hIL-2). The guanine oxidation signal was monitored using differential pulse voltammetry (DPV). It is intended to test the specificity of the sensor using complementary and noncomplementary DNA chains for the hybridization event. The surface properties of CPE and CNTPE and hybridization event on these surfaces were also investigated by electrochemical impedance spectroscopy.

2. EXPERIMENTAL PART

2.1. Regents and Material

Multi-walled carbon nanotubes (CNT) provided by CVD (chemical vapor deposition) method with ~95% purity were obtained from Petroleum and Gas Institute of Iran. Further purification was accomplished by stirring the CNTs in concentrated sulfuric acid. A 20-mer oligonucleotide corresponding to antisense strand of human IL-2 gene (chIL-2) was used as the probe and its complementary (hIL-2) corresponding to sense strand of human IL-2 gene was used as target DNA. ITS1, ITS4, 16SR and P53 oligonucleotides were used as noncomplementary oligonucleotides. All of the oligonucleotides were supplied (as lyophilized powder) by MWG-Biotech company, with the following sequences:

Probe DNA (chIL-2):
5′-CTA AAT TTA GCA CTT CCT CC-3′
Complementary DNA (hIL-2):
5′-GGA GGA AGT GCT AAA TTT AG -3′
Noncomplementary DNAs:
ITS1:
5′-TCC GTA GGT GAA CCT GCG G-3′
ITS4:
5′-TCC TCC GCT TAT TGA TAT GC-3′
16SR:
5′-TAC CTT GTT AGG ACT TCA CC-3′
P53:
5′-AGT TCT CCA TCC CCA-3′

Stock solution of the oligonucleotides (100 μM) were prepared with TE buffer solution (10 mM Tris-HCl, 1 mM EDTA, pH 8.00) and kept frozen. More diluted solutions of the oligonucleotides were prepared using 0.50 M acetate buffer solution (pH 4.80) containing 20 mM NaCl. Other chemicals were of analytical reagent grade. Distilled, deionized and sterilized water was used in all solution preparation. Each measurement consisted of immobilization of probe and detection of target DNA (immobilization/detection cycle) carried out on a fresh CNTPE surface. All the experiments were performed at room temperature in an electrochemical cell.

2.2. Instrumentation

Electrochemical experiments were performed using AUTOLAB PGSTAT 30 electrochemical analysis system and GPES 4.9 software package (Eco Chemie, Netherlands). The utilized three-electrode system was composed of a CNTPE and CPE (surface area of 0.015 cm^2) as the working electrode, a saturated calomel electrode (SCE) as the reference electrode for DPV and $Ag|AgCl|KCl_{3M}$ for EIS methods and a platinum wire as the auxiliary electrode.

2.3. Procedure

2.3.1. Preparation of the Working Electrode

The CNTPE was prepared by mixing CNT, graphite powder and high viscosity paraffin (density = 0.88 g cm^{-3}) from Fluka in a ratio of 10:60:30% (w/w) in a mortar. Unmodified carbon paste electrodes (CPE) were also prepared in a similar way by mixing graphite powder with paraffin oil in a ratio of 70:30% (w/w). A portion of the resulting paste was then inserted in the bottom of a glass tube. The electrical connection was implemented by a copper wire lead fitted into the glass tube. The surface of the resulting paste electrodes were smoothed on a weighing paper and rinsed carefully with distilled water.

2.3.2. Electrochemical Activation of the CNTPE and CPE

The polished electrode was pretreated at optimized potential of 1.80 V vs. SCE for 5 min for electrochemical activation of electrode surface. Pretreatment was carried out in 0.50 M acetate buffer solution (pH 4.80) containing 20 mM of NaCl without stirring.

2.3.3. Immobilization of Probe on the CNTPE and CPE

For immobilization of probe on CPE and CNTPE, following activation, the working electrode was immersed in 0.50 M acetate buffer solution (pH 4.8) containing 1μM probe and 20 mM of NaCl. After that, 0.5 V potential vs. SCE was applied to the electrode for 5 min into the stirred solution (with 200 rpm) at room temperature. Then, the electrode was rinsed with sterilized and deionized water.

2.3.4. Hybridization

Hybridization reaction was conducted by immersing the probe captured electrode into a stirred hybridization solution (0.5 M acetate buffer pH 4.8) containing 3 μM of target oligonucleotide and 20 mM of NaCl, for 5 min, while the electrode potential was held at 0.50 V vs. SCE. The electrode was washed with sterilized and deionized water to remove the non-hybridized DNA. For hybridization of probe with noncomplementary sequences, the same strategy was carried out.

2.3.5. Voltammetric Measurements

Electrochemical investigation was carried out using DPV in 20 mM of Tris-HCl buffer (pH 7.00) solution and scanning the electrode potential between 0.50 and 1.15 V vs. SCE at pulse amplitude of 50 mV.

The raw data were treated using the Savitzky and Golay filter (level 2) of GPES software, followed by the GPES software moving average baseline correction using a "peak width" of 0.01. Repetitive measurements were carried out following renewing the electrode surface by cutting and polishing of the electrode.

2.3.6. Impedance measurement

Surface of the CPE and CNTPE and hybridization event were studied by electrochemical impedance spectroscopy. Impedance measurements were performed in phosphate buffer solution (pH 7.00) containing 1.0 mM $K_4Fe(CN)_6$ / $K_3Fe(CN)_6$ as a redox couple at a potential of 0.22 V (vs. $Ag|AgCl|KCl_{3M}$). The data are represented in the complex plane; Nyquist plots (Z'' vs. Z', Z'' = imaginary impedance and Z' = real impedance). The respective semicircle diameter corresponds to the charge transfer resistance, R_{ct} , the values of which were calculated using the fitting program of AUTOLAB (FRA, version 4.9). The impedance spectra are fitted to a Randles equivalent electrical circuit for CPE and CNTPE with / without the immobilized DNA, including a solution resistance, R_s, a constant phase element (CPE), the charge transfer resistance, R_{ct}, and Warburg impedance, Z_W. From the regression, the charge transfer resistance was obtained.

3. RESULTS AND DISCUSSION

3.1. Preliminary Investigation

The barrier properties of surface of CPE and CNTPE were investigated using electrochemical impedance spectroscopy. Each of the spectra is composed of a semicircle part in a high frequency region and a linear part in a low frequency region, corresponding to the electron transfer process and the diffusion process, respectively. The diameter of the semicircle represents the charge transfer resistance at the electrode surface (R_{ct}). The linear part in impedance spectra represents Warburg

impedance (Z_W) [29]. Nyquist diagrams of $[Fe(CN)_6]^{3-/4-}$ at different electrodes are illustrated in Fig. 1. Curve (a) of this figure represents impedance spectrum at carbon paste electrode modified with carbon nanotubes without any purification. Figure 1b and 1c show impedance spectrum at carbon paste electrode and modified carbon paste electrode with purified CNT, respectively. As shown in this figure, the diameter of the semicircle, indicating the corresponding, R_{ct}, are 13.43×10^3 Ω, 8.75×10^3 Ω and 3.13×10^3 Ω for diagrams a, b and c, respectively. Data comparison clearly shows that charge transfer resistance decreased when carbon paste is mixed with 10% CNT stirred in concentrated sulfuric acid. This difference implies that the pretreatment of CNT with concentrated sulfuric acid for further purification had significant favorable effect on the electrode response. This observation is in accordant with the results reported by other groups indicating that CNT treatment removes metal ions from the nanotube surface which maybe present after their preparation [30]. Furthermore, CNT treatment causes segmentation, carboxylation and opening of terminus [31] and tips of the carbon nanotubes and making them ready to use [32].

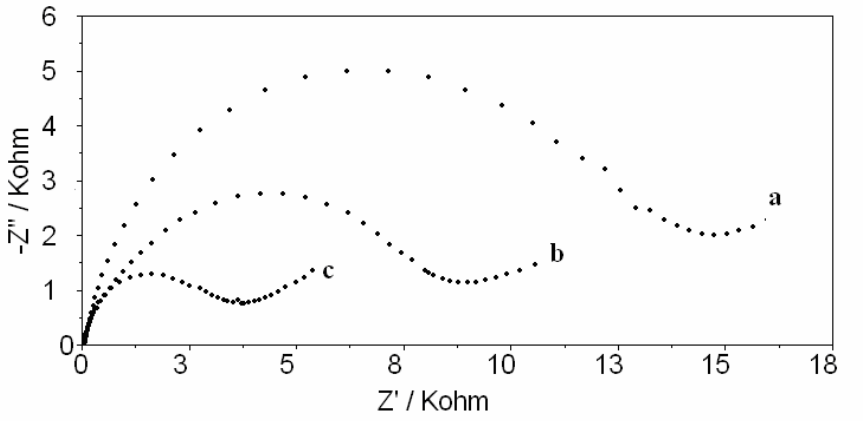

Figure 1. Impedance spectra at modified CPE with impure CNT (a), CPE (b) and CNTPE (modified CPE with purified CNT) (c) in the presence of 1 mM $[Fe(CN)_6]^{3-/4-}$ (1:1) in phosphate buffer (pH 7.00).

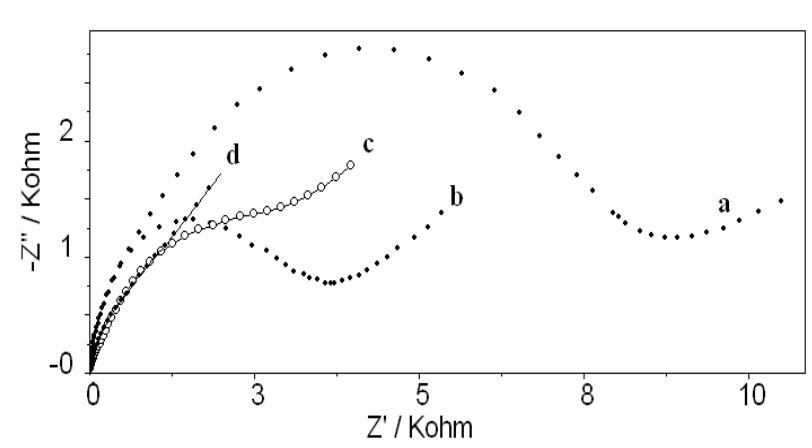

Figure 2. Impedance spectra at (a) CPE before activation, (b) CNTPE before activation, (c) CPE after activation and (d) CNTPE after activation.

Figure 2 shows the impedance spectra at CPE and CNTPE (modified CPE with purified CNT) before (Fig. 2a and b) and after activation of the electrode surface at potential of 1.8 V vs. SCE for 5 min (Fig. 2c and 2d). Comparison of curves a and c of figure 2 indicates that charge transfer resistance decreased from $R_{ct} = 8.75 \times 10^3$ Ω for 2a to $R_{ct} = 1.71 \times 10^3$ Ω for 2c after electrochemical activation of CPE. Figure 2d shows Nyquist diagram at activated CNTPE. It is noticeable that following electrochemically activation of CNTPE surface, charge transfer resistance, semicircle part of impedance diagram, was eliminate and diagram comprises of only linear part (Warburg impedance), meaning that the charge transfer resistance becomes unimportant in relation to Z_w [33]. Because, the surface of CNTPE becomes very electroactive after electrochemical activation and does not repulsive interaction (electrostatic and steric) exist between the redox marker ions and the electrode surface. This linear part of Nyqyst diagram (Warburg impedance, Z_w,) didn't change after probe immobilization and hybridization on the activated CNTPE. Therefore, electrochemical impedance spectroscopy is not suggested as a proper method to study of DNA hybridization event.

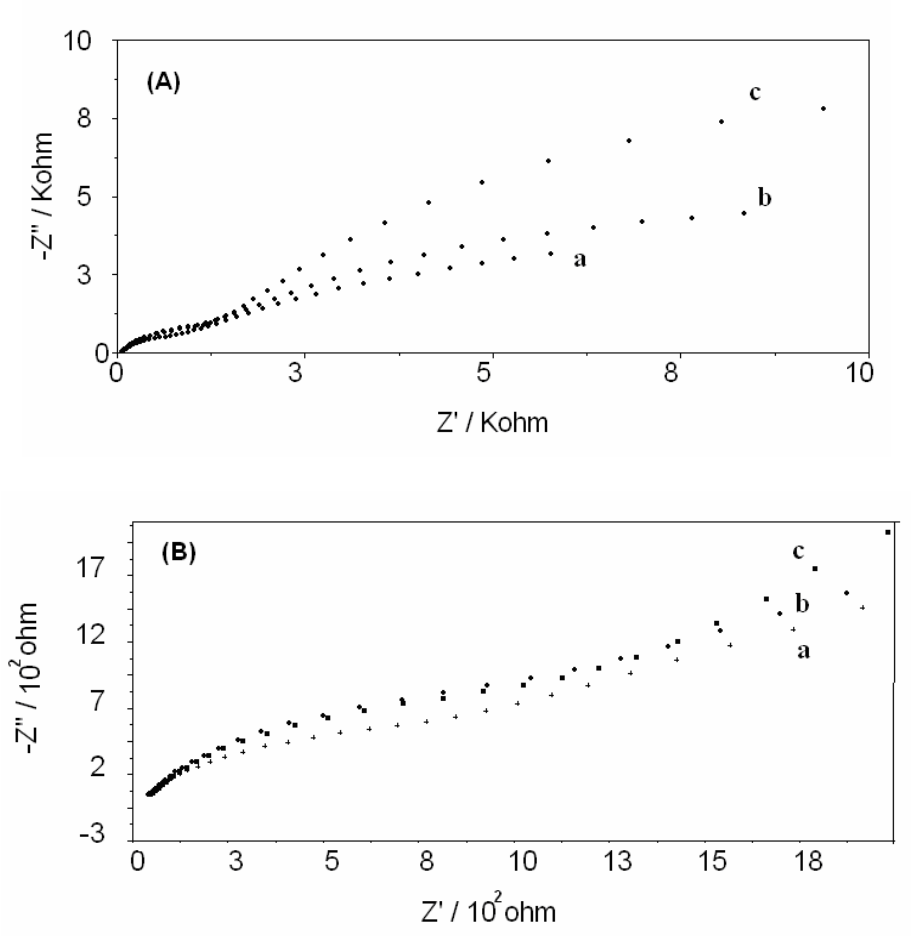

Figure 3. (A) Impedance spectra at (a) activated CPE, (b) after immobilization of hIL-2 probe, and (c) after hybridization. (B) Semicircle part of Fig. 3A: (a) activated CPE, (b) after immobilization of hIL-2 probe, and (c) after hybridization.

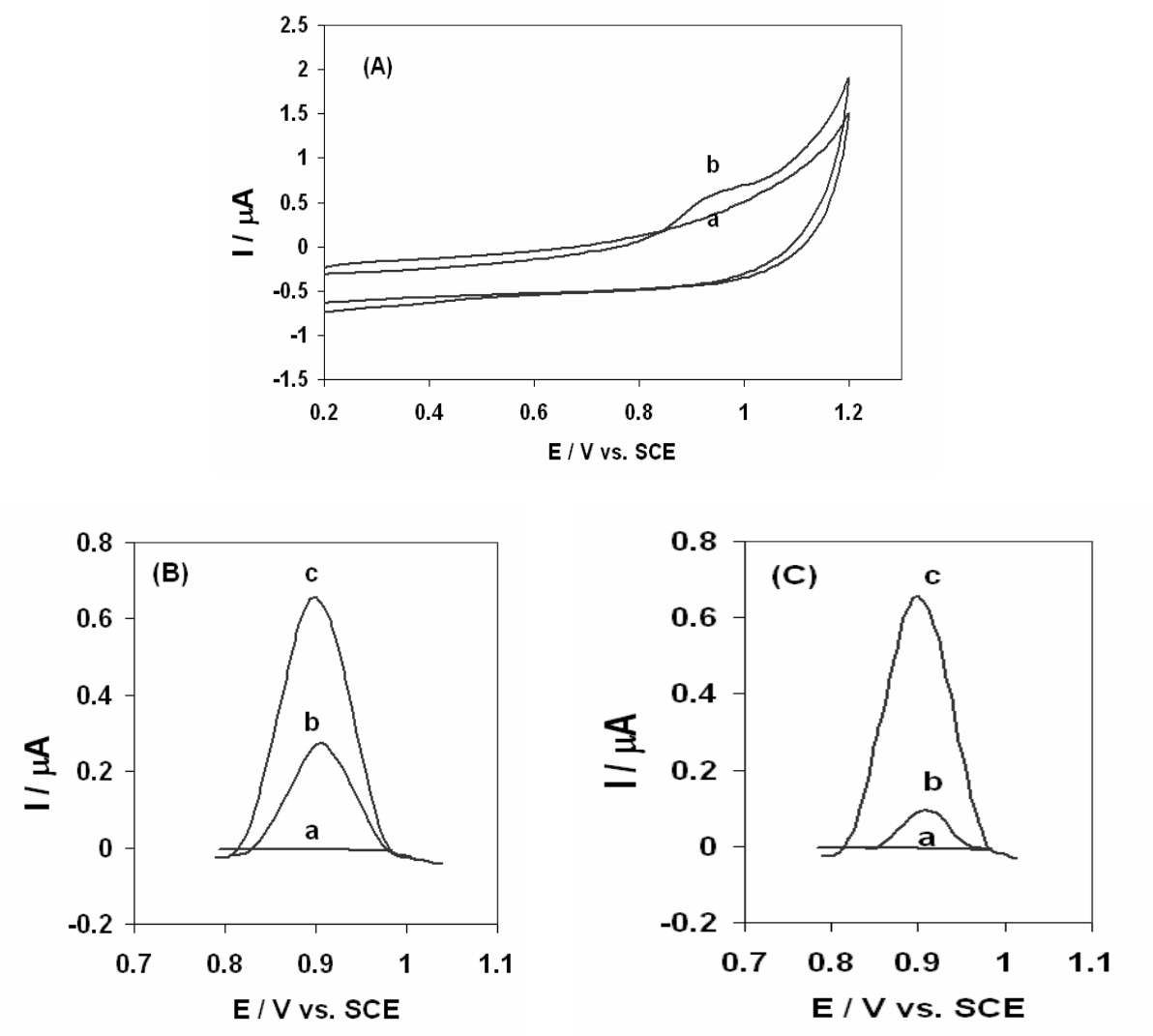

Figure 4. (A) Cyclic voltammograms of bare activated CNTPE (a) and hIL-2 immobilized onto activated CNTPE (b). (B) Differential pulse voltammograms of bare activated CPE and CNTPE (a), hIL-2 immobilized at activated CPE (b) and hIL-2 immobilized at activated CNTPE (c). (C) DPVs of bare activated electrode (a), chIL-2 accumulated onto activated CNTPE (b) and hIL-2 accumulated onto activated CNTPE (c). Electrochemical activation potential was 1.80 V vs. SCE for 5 min and oligonucleotide concentrations in accumulation solution was 1 µM. Other conditions for electrode activation such as oligonucleotides accumulation and voltammetric measurements were as described in Section 2.3.

Figure 3A shows the impedance spectra of activated CPE before immobilization of probe (curve a), after immobilization of chil-2 probe (curve b) and after hybridization with complementary DNA (curve c). The high frequency section of these curves show an arc with a given diameter of 1.71 $\times 10^3$ Ω, 2.72 $\times 10^3$ Ω, 3.69 $\times 10^3$ Ω for curves a, b and c, respectively. Figure 3B shows the difference between semicircle parts of impedance spectra in Fig. 3A with more clarity. It is noticeable that the radius of the semicircular part of the spectrum increases slightly after probe immobilization and

hybridization. The increasing of the diameter of semicircle reflects the increase in the interfacial charge transfer resistance. This is the result of the negative charge of the DNA on the electrode surface decreasing the electron transfer of $[Fe(CN)_6]^{3-/4-}$ marker ion due to electrostatic repulsion. The charge transfer or diameter of semicircular part of the impedance diagram did not clearly increased after probe immobilization and hybridization in the surface of carbon paste electrode compared with other solid electrode such as gold electrode. Because, the surface of the CPE is very porous and probably DNA is trapped in the groves of the surface and less repulsive interactions take place between marker ions and oligonucleotides. These results suggest that detection of DNA hybridization event in the surface of CPE is not beneficial.

The electrochemical behavior of CNTPE was initially investigated by cyclic voltammetry (CV) and DPV for comparing the oxidation signal of guanine, selecting a simple and sensitive electrochemical technique. The cyclic voltammograms of activated bare CNTPE and hIL-2 immobilized activated CNTPE obtained after about 5 min accumulation of hIL-2 at 0.5 V vs. SCE in a 1.0 μM hIL-2 solution into the 20 mM of Tris-HCl buffer solution (pH 7.00) at scan rate of potential 50 mVs^{-1} are shown in Fig. 4A. Figure 4B shows the DPV response of activated bare CNTPE (a), hIL-2 immobilized activated CPE (b) and CNTPE (c). Compression of DPV response of hIL-2 immobilized at the surface of activated CPE and CNTPE shows that the guanine oxidation signal elevated almost 2-fold when CNT was introduced into the CPE; i.e. in CNTPE. The enhanced current values can be attributed to high local density of electronic states in CNT [34]. This observation demonstrated promising potential of CNTPE in increasing guanine signal. Having observed this potential, CNTPE was selected for future experiments.

Before characterization of the system, the electrochemical behavior of chIL-2 and hIL-2 on the CNTPE were investigated separately. These oligonucleotides were immobilized alone on the electrode. Figure 4C shows differential pulse voltammograms obtained for bare activated CNTPE (a), chIL-2 immobilized activated CNTPE (b) and hIL-2 immobilized activated CNTPE (c). As seen in this figure, the peak height of guanine oxidation for hIL-2 (containing 7 guanine) is 0.655 μA ± 0.02, which is about 7 times higher than that of chIL-2 (containing 1 guanine) 0.094 μA ± 0.01. Accordingly chIL-2 was selected as the probe for this study.

3.2 Optimization of the Experimental Variables

Various parameters such as activation potential, activation time and probe immobilization conditions affecting guanine differential pulse voltammetric signal at the CNTPE were examined and optimized.

3.2.1. Influence of Electrochemical Pretreatment of CNTPE

3.2.1.1. Effect of Activation Potential

Electrochemical pretreatment is usually required for activation of the working electrode surface [35]. Electrochemical pretreatment is commonly conducted either at negative or positive potentials

[26]. In this study, potentiostatic method was used for activation of the electrode surface. In order to find an optimum activation potential, the polished CNTPE was activated at different potentials within a wide voltage range (i.e., from -2.0 to 2.5 V vs. SCE) and accumulation of chIL-2 was conducted as described in section 2.3.3. Figure 5A shows the DPV response of chIL-2 immobilized on the activated CNTPE as a probe at imposed potential ranging between -2.0 and 2.5 V vs. SCE. As seen in this figure, activity of the electrode improved when potentials exceeded from 1.0 V vs. SCE until reached to its maximum value at 1.80 V vs. SCE and then decreased at more positive potentials. When potential was higher than 2.0 V vs. SCE or lower than -1.5 V vs. SCE, the oxidation or reduction of supporting electrolyte ions or solvent itself was occurred. In voltages higher than 2.0 V vs. SCE, gaseous products were observed significantly at the surface of working electrode that could damage CPE and CNTPE.

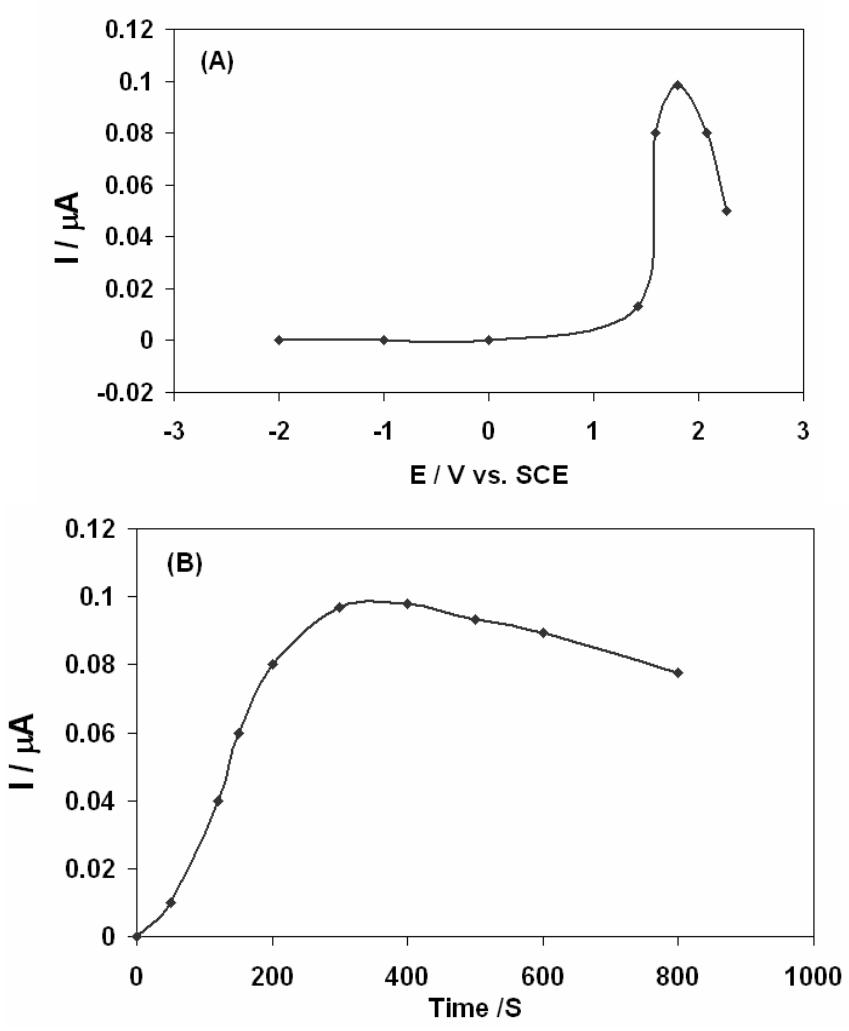

Figure 5. Variations of DPV signal of the immobilized hIL-2 on the activated CNTPE vs. activation potentials (A) and activation times (B). The concentration of hIL-2 in solution was 1 µM, other conditions for CNTPE activation, hIL-2 immobilization and DPV measurements as described in section 2.3.

3.2.1.2. Effect of Activation Time

In order to optimize activation time of the working electrode, different activation time periods were used. The accumulation of chIL-2 on the electrode was performed according to the procedure described in section 2.3.3. Figure 5B displays the DPV response of chIL-2 versus activation time. As seen in this figure, the chIL-2 signal was increased with increasing the activation time and nearly leveled off after 10 min. These results demonstrated that about 5 min is adequate and optimum time for activation of the CNTPE surface in order to accumulate almost maximum amount of chIL-2 probe.

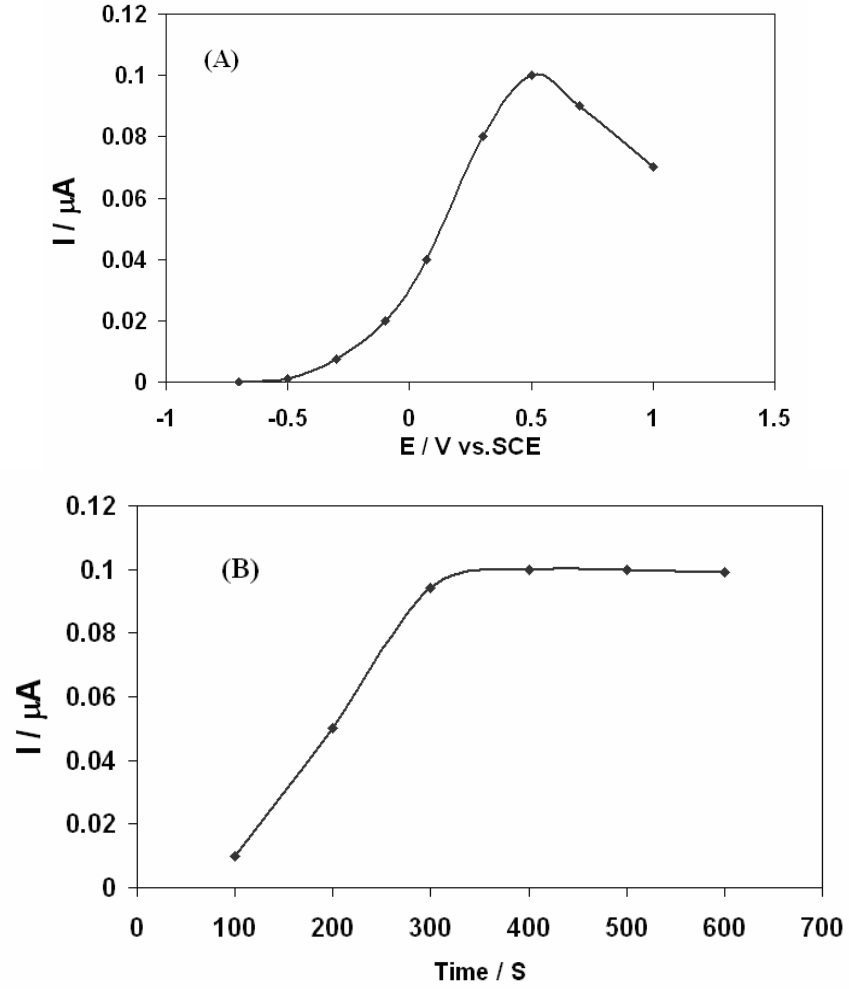

Figure 6. The variations of DPV response of immobilized hIL-2 oligonucleotide on the activated CNTPE vs. immobilization potential (A) and immobilization time (B). The concentration of hIL-2 was 1µM and other conditions as described in section 2.3.

3.2.2. Immobilization Conditions of Probe on the CNTPE

3.2.2.1. Effect of Immobilization Potential

Considering that adsorption and immobilization of the probe on the electrode surface is very important for DNA biosensors function, and on the other hand, accumulation of DNA probes is

influenced by the imposed potential to the electrode during the accumulation, the influence of imposed potential on the electrochemical behavior of chIL-2 was investigated using DPV. For this, we studied the imposed potentials ranging between -0.80 and 0.8 V vs. SCE (Fig. 6A). As shown in the figure, the potential around 0.50 V vs. SCE was obviously favorable for obtaining the maximum peak current for oxidation of guanine. Therefore, potential of 0.50 V vs. SCE was selected as optimum immobilization potential.

3.2.2.2. Effect of Immobilization Time

The effect of immobilization time of the probe on the activated CNTPE was studied using DPV. Figure 6B shows DPV signal of chIL-2 versus the immobilization time. As can be seen, the amount of adsorbed DNA rises with increasing adsorption time and starts to saturate at approximately 300s. Accordingly, all further experiments were carried out with an immobilization time of 300 s.

3.3. Electrochemical Detection of Hybridization

Electrochemical detection of DNA hybridization was monitored by differential pulse voltammetry. Once immobilization of the probe on the activated CNTPE was achieved, the electrode was immersed in target DNA solution as described in section 2.3.4. Having formed DNA duplex chain, two opposed events in relation with magnitude of the probe guanine oxidation signal take place. These events which are in competition with each other include: I) the electrochemical signal of the probe's free guanine bases is decreased upon hybridization with complementary cytosine bases on the target DNA. This is because of less availability of guanine bases in the hybrid form for oxidation [36]. II) The electrochemical signal of guanine bases is increased due to increase of the number of total guanine bases in double-stranded DNA in comparison to single-stranded-DNA. This problem is solved by using inosine-modified (guanine-free) probes [36-38]. This is because, although inosine moiety forms a specific base-pair bond with cytosine residue [39], but is almost electroinactive [37, 40]. Indeed, the duplex formation is detected through the appearance of the target DNA's guanine oxidation signal, following hybridization. The main disadvantage of this approach is the lack of an electrochemical signal of the probe for direct follow up probe's signal and optimizing its immobilization conditions.

One of the beneficial strategies is to use a probe which contains preferably only one or few guanine bases with several cytosines. Importance of the presence of only one guanine base relies on possibility of probe immobilization monitoring and consequently possibility of optimization of probe immobilization on the electrode [24, 25, 41]. Several cytosine bases in the probe are useful for hybridization with target DNA that contains several guanine bases. On the basis of this approach guanine oxidation signal remarkably increases after hybridization of probe with DNA target and therefore, can be easily recorded. Short DNA sequences related to human IL-2 gene (chIL-2) used in this study was designed according to this strategy.

Figure 7 displays the DPV at activated CNTPE (A) and CPE (B) following immobilization of chIL-2 as the probe (a), and after hybridization with hIL-2 as target DNA (f). As shown in this figure,

the guanine signal of the probe-complementary DNA hybrid was 0.26 μA for CNTPE and 0.11 μA for CPE which are more than 2-fold higher than those of probe alone.

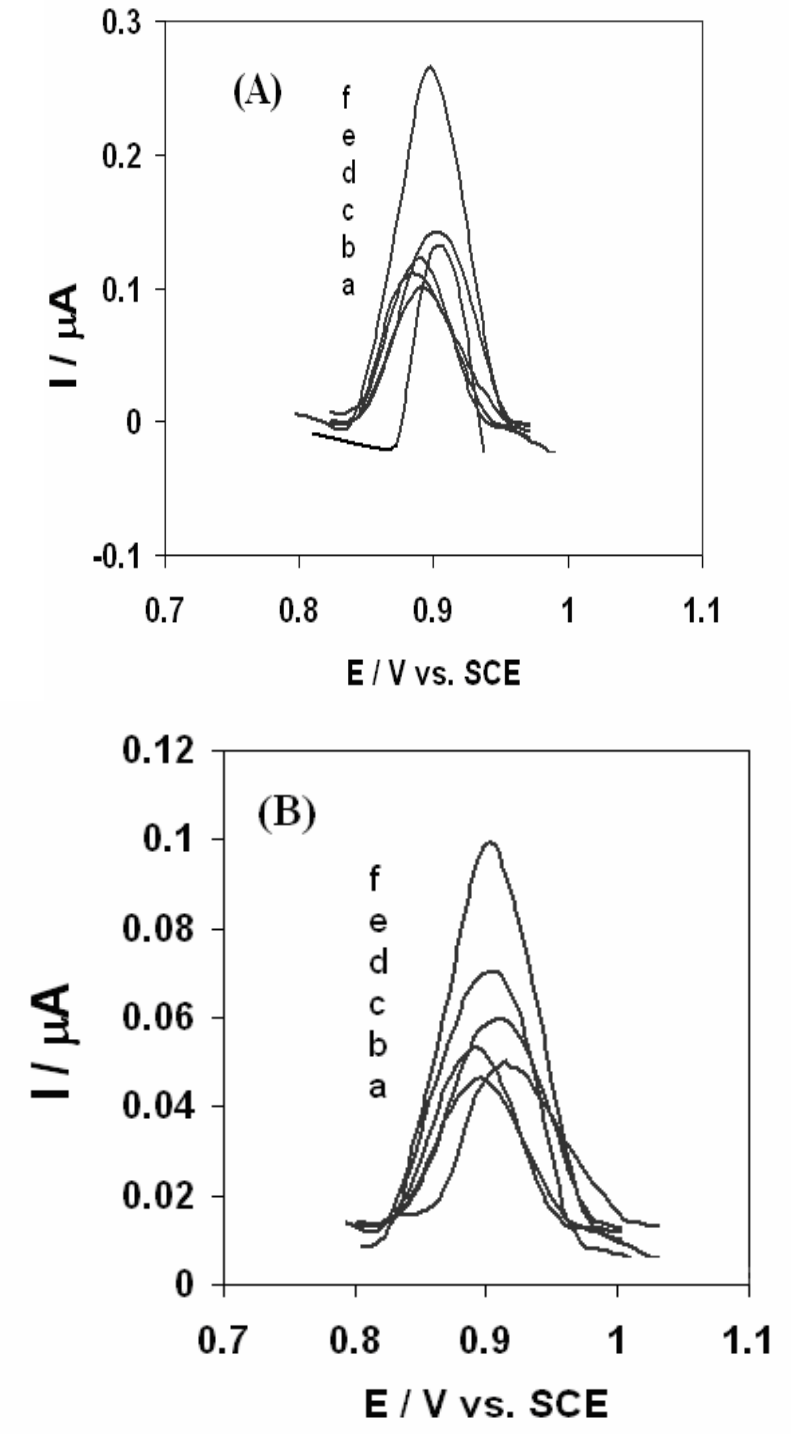

Figure 7. DPVs of chIL-2 modified CNTPE (A) and chIL-2 modified CPE (B) before hybridization (a) and after hybridization with: hIL-2 target oligonucleotide (3 μM) (f); after hybridization with 3 μM noncomplementary oligonucleotides P53 (b), 16SR (c), ITS4 (d) and ITS1 (e). Probe concentration in accumulation solution was 1.0 μM. Experimental conditions were as cited in Fig.4 and described in section 2.3.

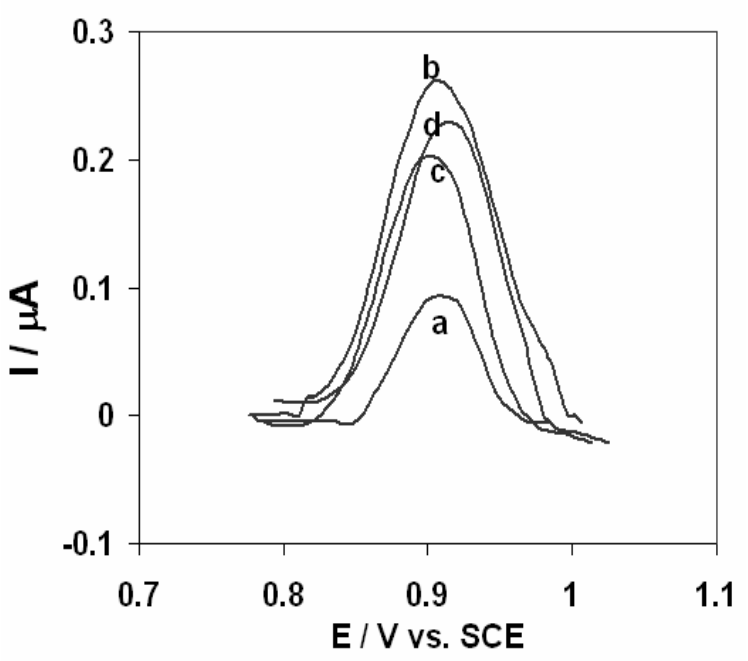

Figure 8. Differential pulse voltammograms of chIL-2 modified activated CNTPE before hybridization (a), after hybridization with hIL-2 target in a sample containing: (b) only hIL-2 oligonucleotide, (c) both hIL-2 and ITS4 (d) both hIL-2 and ITS1. Experimental conditions were as cited in Fig. 7.

3.4. Selectivity Study

The selectivity of hybridization detection of the proposed DNA sensor to the target was studied via performance of some hybridization experiments with noncomplementary oligonucleotides. For this purpose four different oligonucleotides P53, 16SR, ITS4 and ITS1 containing 1, 3, 3 and 7 free guanine bases, respectively, were selected as noncomplementary DNAs (Fig. 7b, c, d and e). As shown in this figure, the interaction between these noncomplementary oligonucleotides and chIL-2 modified activated CNTPE did not lead to a significant increase in the guanine oxidation signal because hybridization of the probe with the DNAs did not carry out entirely. However, guanine signal increased slightly that may be attributed to the negligible adsorption of the noncomplementary oligonucleotides to some free sites present on the activated CNTPE or due to short and non-complete hybridization between the probe and non-complementary DNAs. This slight increasing is ordered with their guanine base numbers.

The DNA sensor selectivity was also investigated in samples containing both complementary (hIL-2) and noncomplementary sequences. Figure 8 displays the DPV for probe modified activated CNTPE before hybridization (a) and after hybridization with hIL-2 (b), in binary mixture of hIL-2 and ITS4 (c), in binary mixture of hIL-2 and ITS1 (d). As illustrated, the interactions between hIL-2 and ITS1 or ITS4 in the mixture solution have less effect on the hybridization event between probe and hIL-2 target. However guanine signal decreases slightly, probably because of partial hybridizations

occurred between the probe and non-complementary DNAs and also between target and noncomplementary oligonucleotides in their mixture solution. These interactions give rise to a slight decrease in availability and hybridization between target DNA and immobilized probe.

The results of selectivity study revealed that only complementary hIL-2 as the target DNA can form an effective duplex with chIL-2 as the probe and consequently causes a significant increase in guanine oxidation signal.

4. CONCLUSIONS

Carbon paste electrodes possess advantages of ease of preparation and easy renewable of surface. The results suggest a label–free DNA hybridization biosensor based on activated CNTPE using differential pulse voltammetry. This study demonstrated that CNTPE had some advantages over CPE. Utilization of carbon nanotubes as incorporated particles into a carbon paste electrode improves the electrochemical signal of this biosensing procedure. The enhanced current values can be attributed to the high local density of the electronic states in CNT. The proposed biosensor eliminates time consuming external indicator accumulation and selectively responses to the target complementary DNA. The hybridization event on CPE surface by EIS was not clearly detected and on CNTPE surface was not possible.

References

1. M. Ligaj, J. Jasnowska, W.G. Musial, M. Filipiak, *Electrochim. Acta,* 51 (2006) 5193.
2. J. Watterson, P.A.E. Piunno, U.J. Krull, *Anal.Chim. Acta*, 469 (2002) 115.
3. M. Yang, M.E. McGovem, M. Thompson, *Anal.Chim. Acta*, 346 (1997) 259.
4. O.A. Arotiba, A. Ignaszak, R. Malgas, A. Al-Ahmad, P.G.L. Baker, S.F. Mapolie, E.I. Iwuoha, *Electrochim. Acta*, 53 (2007) 1689.
5. P. de-los-Santos-Alvarez, M.J. Lobo-Castanon, A.J. Miranda-Ordieres, P. Tunon-Blanco, *Anal. Bioanal. Chem.*, 378 (2004) 104.
6. X. Sun, P. He, S. Liu, L.Ye, Y. Fang, *Talanta,* 47 (1998) 487.
7. C. Ge, W. Miao, M. Ji, N. Gu, *Anal Bioanal Chem,* 383 (2005) 651.
8. J. Chen, J. Zhang, Q. Zhuang, J. Chen, X. Lin, *Electrochim. Acta*, 53 (2008) 2716.
9. N. Zhu, Z. Chang, P. He, Y. Fang, *Electrochim. Acta,* 51 (2006) 8758.
10. G. Li, N. Liu, S. Liu, S. Zhang, *Electrochim. Acta*, 53 (2008) 2870.
11. K. Wu, J. Fei, W. Bai, S. Hu, *Anal. Bioanal. Chem.* 376 (2003) 205.
12. Y.D. Zhao, D.W. Pang, S. Hu, Z.L. Wang, J.K. Cheng, H.P. Dai, *Talanta*, 49 (1999) 751.
13. C.Jiang, T. Yang, K. Jiao, H. Gao, *Electrochim. Acta,* 53 (2008) 2917.
14. J. Wang, J.R. Fernandes, L.T. Kubota, *Anal. Chem.*, 70 (1998) 2943.
15. K.H.W. Kroto, J. R. Heath, S.C. O′Brien, R.F. Curl, R.E. Smalley, *Nature* 318 (1985) 162.
16. S. Iijima, *Nature*, 354 (1991) 56.
17. R.H. Baughman, A. Zakhidov, W.A. de Heer, *Science,* 297 (2002) 787.
18. J. Wang, A. Kawde, M. R. Jan, *Biosens. Bioelectr.*, 20 (2004) 995.
19. ML. Pedano, GA. Rivas, *Electrochem. Commun,* 6 (2004) 10.
20. MD. Rubianes, GA. Rivas, *Electrochem. Commun,* 5 (2003) 689.

21. D. Xu, D.W. Xu, X. Yu, Z. Liu, Z. He, Z. Ma, *Anal. Chem*., 77 (2005) 5107.
22. Y. Xu, Y. Jiang, H. Cai, P.G. He, Y.Z. Fang, *Anal. Chim. Acta*, 516 (2004) 19.
23. J. Yang, T. Yang, Y. Feng, K. Jiao, *Anal. Biochem*., 365 (2007) 24.
24. M.H. Pournaghi-Azar, M.S. Hejazi, E. Alipour, *Anal. Chim. Acta*, 570 (2006) 144.
25. M.H. Pournaghi-Azar, M.S. Hejazi, E. Alipour, *Electroanal.*, 19 (2007) 466.
26. M.S. Hejazi, E. Alipour, M.H. Pournaghi-Azar, *Talanta,* 71 (2007) 1434.
27. M.H. Pournaghi-Azar, E. Alipour, S. Zununi, H. Froohandeh, M.S. Hejazi,, Biosens. Bioelectr., 24 (2008) 524.
28. M.S. Hejazi, M.H. Pournaghi-Azar, E. Alipour, F. Karimi, Biosens. Bioelectr., 23 (2008) 1588.
29. T.H. Degefa, J. Kwak, *J. Electroanal. Chem*., 612 (2008) 37.
30. N.S. Lawrence, R.P. Deo, J. Wang, *Talanta*, 63 (2004) 443.
31. K. Wu, J. Fei, W. Bai, S. Hu, *Anal. Bioanal. Chem.*, 376 (2003) 205.
32. X. Lin, J. He, Z. Zha, *Sens. Actuat., B*, 119 (2006) 608.
33. H. Peng, C. Soeller, N. Vigar, P. Kilmartin, M. Cannell, G. Bowmaker, R. Cooney, J. Sejdic, *Biosens. Bioelectr.,* 20 (2005) 1821.
34. S.Timur, U. Anik, D. Odaci, L. Gorton, *Electrochem. Commun.,* 9 (2007) 1810.
35. R.L. Mc Creery, K.K. Cline, in: Kissinger, W.R. Heineman (Eds.), Laboratory Techniques in Electroanalytical Chemistry, second ed., Marcel Dekker, 1996 (Chapter 10).
36. J. Wang, G.Rivas, J.R. Fernandes, J.L. lopez Paz, M. Jiang, R. Waymire, *Anal. Chim. Acta,*. 375 (1998) 197.
37. J. Wang, A.N. Kawde, A. Erdem, M. Salazar, *Analyst*, 126 (2001) 2020.
38. F. Lucarelli, G. Marrazza, I. Palchetti, S. Cesaretti, M. Mascini, *Anal. Chim. Acta*., 469 (2002) 93.
39. S. Casegreen, E. Southern, *Nucleic Acids Res*., 22 (1994) 131.
40. P. Kara, D. Ozkan, A. Erdem, K. Kerman, S. Pehlivan, F. Ozkinay, D. Unuvar, G. Itili, M. Ozsoz, *Clin. Chim. Acta,* 336 (2003)57.
41. R.E. Sabzi, B. Sehatnia, M.H. Pournaghi-Azar, M.S. Hejazi, *J. Iran. Chem. Soc*., 5 (2008) 476.